HHS Public Access

Author manuscript

Mol Pharm. Author manuscript; available in PMC 2020 June 03.

Published in final edited form as:

Mol Pharm. 2019 June 03; 16(6): 2445–2451. doi:10.1021/acs.molpharmaceut.9b00059.

Evaluation of Targeting Efficiency of Joints with Anticollagen II Antibodies

Laren A. Lofchy[†,‡,#], **Vivian P. Vu**[†,#], **Nirmal K. Banda**[§,‖], **Joseline Ramos Ramirez**[§], **Weston J. Smith**[†], **Geoffrey Gifford**[†], **Hanmant Gaikwad**[†], **Robert I. Scheinman**[‖,⊥], **Dmitri Simberg**[*,†,‖,⊥]

[†]Translational Bio-Nanosciences Laboratory, The Skaggs School of Pharmacy and Pharmaceutical Sciences, University of Colorado, Anschutz Medical Campus, Aurora, Colorado 80045, United States

[‡]Graduate Program in Pharmaceutical Sciences, The Skaggs School of Pharmacy and Pharmaceutical Sciences, University of Colorado, Anschutz Medical Campus, Aurora, Colorado 80045, United States

[§]Division of Rheumatology, School of Medicine, University of Colorado Denver, Anschutz Medical Campus, Aurora, Colorado 80045, United States

[‖]Colorado Center for Nanomedicine and Nanosafety, The Skaggs School of Pharmacy and Pharmaceutical Sciences, University of Colorado, Anschutz Medical Campus, Aurora, Colorado 80045, United States

[⊥]Department of Pharmaceutical Sciences, The Skaggs School of Pharmacy and Pharmaceutical Sciences, University of Colorado, Anschutz Medical Campus, Aurora, Colorado 80045, United States

Abstract

Diseases of the joints affect over 10% of the world's population, resulting in significant morbidity. There is an unmet need in strategies for specific delivery of therapeutics to the joints. Collagen type II is synthesized by chondrocytes and is mainly restricted to the cartilage and tendons. Arthrogen-CIA is a commercially available anti-collagen II antibody cocktail that reacts with 5 different epitopes on human, bovine, and mouse collagen II. Arthrogen has been used for induction of experimental rheumatoid arthritis (RA) in mice because of high complement activation on the cartilage surface. Native collagen II might serve as a useful target for potential delivery of therapeutics to the joint. To evaluate the efficiency and specificity of targeting collagen II, Arthrogen was labeled with near-infrared (NIR) dye IRDye 800 or IRDye 680. Using ex vivo

[*]**Corresponding Author:** dmitri.simberg@ucdenver.edu.

[#]Author Contributions

L.A.L. and V.P.V. contributed equally to this work.

The authors declare no competing financial interest.

ASSOCIATED CONTENT

Supporting Information

The Supporting Information is available free of charge on the ACS Publications website at DOI: 10.1021/acs.molpharmaceut.9b00059.

Linearity of dot blot assay and layout of the organs and the corresponding fluorescent scans (composite 700 and 800 nm) for the experiment in Figure 2D (PDF)

NIR imaging, we demonstrate that Arthrogen efficiently and specifically accumulated in the limb joints regardless of the label dye or injection route (intravenous and subcutaneous). After subcutaneous injection, the mean fluorescence of the hind limb joints was 19 times higher than that of the heart, 8.7 times higher than that of the liver, and 3.7 times higher than that of the kidney. Control mouse IgG did not show appreciable accumulation. Microscopically, the antibody accumulated on the cartilage surface of joints and on endosteal surfaces. A monoclonal antibody against a single epitope of collagen II showed similar binding affinity and elimination half-life, but about three times lower targeting efficiency than Arthrogen in vitro and ex vivo, and about two times lower targeting efficiency in vivo. We suggest that an antibody against multiple epitopes of collagen II could be developed into a highly effective and specific targeting strategy for diseases of the joints or spine.

Graphical Abstract

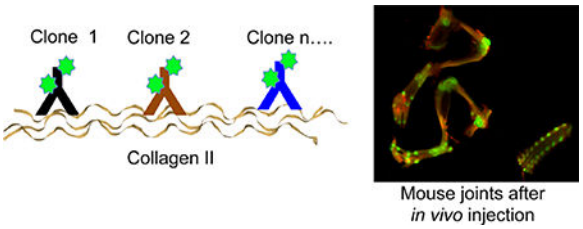

Keywords

cartilage; joint; targeting; arthritis; antibody; collagen; near infrared fluorescence

INTRODUCTION

Joint disease is a common affliction. Studies of rheumatic disease prevalence have found that the numbers of affected individuals in the US have increased from an estimated 21 million in 1995 to 27 million in 2007.[1] This correlates with the aging of the population and with the increase in obesity. For the majority of joint diseases, localized treatments [e.g., intraarticular (IA) and tendon injections] are not always feasible because of limited accessibility, cost, and complication.[2,3] At the same time, some systemic therapies (e.g., glucocorticoids, TNF-α inhibitors, B-cell depletion, and methotrexate) cause substantial immunosuppression and morbidity.[4–6] Therefore, there is a substantial effort directed toward the development of specific, targeted therapies of the joints.

Collagen type II is composed of fibrils of the COL2A1 gene product. It is primarily found in the extracellular matrix of articular collagen and is also found in intervertebral discs, the vitreous humor of the eye,[7] and tendons.[8] Several groups reported development of single-chain antibodies (scFv) and peptides targeting modified collagen II.[9–12] Some of these reagents showed modest binding affinity of low μM to high nM.[11] Although the presence of degraded and denatured collagen II in the diseased and aged joints has been demonstrated,[13–15] it is not very abundant in the joints with mild disease;[14] therefore, native collagen presents an attractive target for drug delivery. Arthrogen-CIA contains a mixture of five IgG2 antibody clones raised against different collagen II epitopes and selected for the

optimal induction of experimental rheumatoid arthritis (RA) in mice.[16] Upon injection of very large doses of Arthrogen (6 mg/mouse) followed by booster lipopolysaccharide, there is a highly efficient development of RA with a characteristic clinical presentation quite similar to that seen in human RA.[16] The main trigger of disease requires two events: binding of IgG to the cartilage and efficient complement fixation via the alternative and the lectin pathways.[17,18] Complement plays an important role in the initiation and evolution of both RA[19] and osteoarthritis (OA).[20] Downstream complement cleavage products C3a and C5a trigger chemotaxis and activation of neutrophils and monocytes, whereas membrane attack complex C5b–C9 causes cell damage. Consistent with this, the IgG2 antibody isotype is one of the most efficient at fixing complement.

Several lines of evidence suggest a better targeting efficiency of antibody cocktails versus single clone antibodies for variety of applications.[21,22] Here, ignoring the complement fixation properties of Arthrogen and focusing instead on its binding properties, we sought to comprehensively characterize the body distribution and targeting efficiency of Arthrogen after systemic and subcutaneous injection using near infrared (NIR) imaging. The results demonstrate a highly efficient and rapid accumulation in the joints in mice, which was superior to a single clone anticollagen II antibody. This opens up possibilities for specific imaging and therapeutic delivery targeted to collagen II with nonpathogenic antibodies.

MATERIALS AND METHODS

Materials

Arthrogen-CIA 5-clone cocktail (catalog number 53040) and single clone antibody against CB11 epitope of collagen type II (clone 35, catalog number 7048) were obtained from Chondrex, Inc. (Redmond, WA, USA) and stored in aliquots at −20 °C before use. The goat anti-C3 antibody (horseradish peroxidase conjugated) was from MP Biomedicals (Solon, OH, USA). IRDye 800CW-NHS ester and IRDye 680RD-NHS ester were from Li-COR (Lincoln, NB, USA). Purified mouse IgG was from Jackson ImmunoResearch (West Grove, PA, USA). Proteinase K solution was from Qiagen. A bovine type II collagen from newborn calves (cat # CJ385) was obtained from Elastin Products Company, Inc. (Owensville, MO, USA). Antibodies were labeled by incubation with a 10-fold excess of dye for 5 h at 4 °C in phosphate-buffered saline (PBS). Unbound dye was removed with a 7 kDa Zeba desalting column (Thermo Fisher). Antibodies were resuspended in sterile PBS and stored at 4 °C before use.

Mouse Experiments

The University of Colorado Institutional Animal Care and Use Committee (IACUC) approved all animal experiments (protocol 103913(11)1D). Mice were treated according to regulations provided by the Office of Laboratory Animal Resources at the UC. Wild-type BALB/c mice were bred in house.

In order to determine the circulation half-life of NIR-labeled antibodies, 2 μL of plasma collected at different time points was applied in triplicates on a 0.22 μm nitrocellulose membrane and scanned at 800 and 700 nm using Li-COR Odyssey. The spot-integrated

density of a 16-bit TIFF image was measured with ImageJ, expressed as a percentage of 1 min time point, and plotted as a function of time using Prism (GraphPad, San Diego CA). The plasma terminal (slow phase) half-life was calculated by fitting into a two-compartment decay curve.

For organ distribution, Ab-injected and control mice were sacrificed and the organs were placed in wells of a 24-well plate (transparent bottom). Bones were cleaned of muscle and sandwiched between two glass slides. Organs and bones were scanned with a Li-COR Odyssey at both wavelengths (700 nm channel for autofluorescence or IRDye 680 and 800 nm channel for IRDye 800). Mean fluorescence was determined from 16-bit images using ImageJ software by subtracting the background, drawing an region of interest around the organs, and using a measure function to determine the mean gray value. When only IRDye 800 was used, the 700 nm channel intensity (red) was artificially enhanced in order to provide an autofluorescent background (outline) of the organs in the images.

Bone Digestion

After scanning, all of the limbs were cleaned of residual muscle. The knee and elbow joints, including about 2 mm of the bone above and below the joint, were cut out with a scalpel. The individual joints were placed in separate 2 mL tubes with screw-on caps, and 400 μL of 100 mM ethylenediaminetetraacetic acid (EDTA) (pH 7.5) plus 2–3 zirconium beads was added. The bones were homogenized with a Mini-BeadBeater tissue disruptor (BioSpec Products, Bartlesville, OK) for 3 cycles of 2 min each. After homogenization, 20 μL of proteinase K solution (Qiagen) was added and samples were mixed at maximum speed at 55 °C using a ThermoMixer (Eppendorf) for 3 h or until the liquid was clear. The dilutions of antibody used for standards were generated in the lysate of control non-injected joints. The samples and the standard dilutions were dotted (2 μL) in triplicates on a nitrocellulose membrane (Bio-Rad), and the dots were scanned with a Li-COR Odyssey at 800 nm. The dots' integrated densities in the TIFF image were measured with ImageJ software, and the amount of IgG in the joints was calculated.

NIR Microscopy

After the antibody cleared from circulation, bones were harvested and the muscle tissue was removed. Bones were placed in 4% formalin solution for 2 days, followed by 2 mM EDTA solution for 1 week. This procedure softens the bone for subsequent microtome cutting. The bones were placed in optical coherence tomography, frozen at −80 °C, and cut with a Leica cryostat at 10 μm thickness in longitudinal sections. At least 10 slides per each bone were prepared. Slides were washed briefly with PBS, the Hoechst solution was added, and bones were imaged with a Zeiss Axio Observer 5 epifluorescent microscope equipped with X-Cite 200DC light source and Axiocam 506 monochromatic camera. NIR fluorescence was imaged with a Cy7 filter set, catalog number 49007, Chroma Corporation (McHenry, IL, USA).

Collagen II Binding Assay

A stock solution of bovine collagen type II was prepared by diluting 100 mg of collagen in 25 mL of cold 0.01 M acetic acid and stored at −70 °C prior to use as previously described.

[23] A transparent bottomed, black 96-well plate (Greiner) was coated with 50 μL of collagen II solution diluted to a concentration of 50 μg/mL in 0.1 M sodium bicarbonate buffer pH 9.3 and incubated overnight at 4 °C. Control plates were coated with 1% bovine serum albumin (BSA). The next day, plates were washed four times with 50 μL of 0.05% Dulbecco's PBS-Tween 20 and blocked with 1% BSA at room temperature for 1 h and washed. Plates were stored at 4 °C before use. The NIR dye-labeled antibody was added at different concentrations and incubated at room temperature for 2 h. The plate fluorescence was read with a Li-COR Odyssey scanner at 800 nm, and the integrated density of gray 8-bit images (TIFF) of the wells was determined with ImageJ software. The intensities were plotted against log-transformed concentrations, and the data were fitted into a dose-response curve in order to calculate EC_{50} with Prism 6.0.

Ex Vivo Binding Assay

Femurs, tibia, and fibula were harvested from three 6-week-old male BALB/c mice and were cleaned of muscle tissue. Bones were placed in a solution of either 1 μg/mL Arthrogen-800 or 1 μg/mL CB11–800 in 1× PBS/1% BSA and shaken at 350 rpm for 1 h at room temperature in a ThermoMixer (Eppendorf). Bones were then removed from the antibody solutions and washed five times with 1× PBS/0.1% Tween 20. Bones were then placed between glass slides, and near-infrared fluorescence images were taken with a Li-COR Odyssey. The relative fluorescence intensity was quantified with ImageJ.

RESULTS

Arthrogen CIA has been developed for induction of collagen antibody-induced arthritis.[16,19] It contains 4 clones of IgG2a and 1 clone of IgG2b, all of them directed against the CB11 fragment (CII 124–402) of type II collagen (Figure 1A). In order to enable imaging of the antibody targeting in vivo, we labeled Arthrogen with IRDye 800 (Figure 1B), which is a popular fluorophore for NIR imaging and currently in clinical development.[24] The fluorophore per antibody ratio was kept between 2 and 4 throughout this study, and the label did not affect the running pattern on sodium dodecyl sulfatepolyacrylamide gel electrophoresis (SDS-PAGE) (Figure 1C).

We injected iv 50 μg of Arthrogen-IRDye 800 (Arthrogen-800) or 50 μg of mouse IgG (polyclonal antibody labeled with ~6 IRDye 680/IgG) into separate mice, or equimolar mixture of 25 μg Arthrogen-800 and mIgG-680 into the same BALB/c mouse. Plasma levels of both antibodies were measured with a fluorescent dot blot assay, which is highly linear as demonstrated in Figure S1 and in our previous publications.[25–27] According to Figure 2A, Arthrogen had a shorter half-life than IgG (36 and 101 h, respectively). At day 22 post-injection (less than 0.1% of the injected antibodies remained in the circulation), mice were dissected and the organs and bones were scanned with a Li-COR Odyssey. As shown in Figure 2B, Arthrogen localized to the joints in the hind limbs, forelimbs, and the spine. Control IgG did not show any evidence of localization in the joints, and the IRDye 680 signal was very low (Figure 2B, upper right). In mice injected with both antibodies, the difference in biodistribution was even more obvious with joint regions highlighted in green (Figure 2B, lower left).

In order to exclude the role of dye in the observed targeting efficiency, the dyes were swapped: Arthrogen was labeled with IRDye 680, and mouse IgG was labeled with IRDye 800. BALB/c mice were injected iv with 40 μg of antibody, and the accumulation in the main organs and joints was studied at 24 h and 22 days post-injection. This time, Arthrogen showed longer half-life than IgG (64 vs 37 h, respectively Figure 2C), strongly suggesting that the type of the label influences the pharmacokinetics of the antibody. Arthrogen-680, but not IgG-800, showed efficient and specific accumulation in the joints and the spine, with almost no accumulation in skin and major organs at both early and late time points (Figures 2D and S2). Thus, although the label affects the pharmacokinetics of the antibodies, it does not affect the targeting specificity.

For the majority of chronically administered therapeutic antibodies, subcutaneous injection is the preferred administration route because it can typically be self-administered.[28,29] We labeled both Arthrogen and mouse IgG with IRDye 800 and injected subcutaneously (40 μg in 40 μL of PBS) into separate BALB/c mice. The use of the same dye allowed for direct comparison of accumulation of targeted and control antibodies without the confounding effect of the dye chemistry. According to the fluorescent images of bones and main organs (Figure 3A,B) and mean fluorescence quantification (Figure 3C) 21 days post-injection, there was on average 4.7 times higher mean fluorescence in the joints of the Arthrogen-800 injected mouse than the mIgG-800 injected mouse. Arthrogen mean fluorescence in other organs was much less (Figure 3B). As shown in Figure 3C, the mean fluorescence of control organs was higher for IgG-800 than that for Arthrogen-800. Additionally, mean fluorescence of the joints in Arthrogen-800 injected mice was much higher than that of other organs. The mean fluorescence in the hind limbs was 19 times higher than that in the heart, 8.7 times higher than that in the liver, and 3.7 times higher than that in the kidney. These data suggest that following subcutaneous injection Arthrogen preferentially targets the joints with minimal deposition in other organs.

In order to quantify the absolute amount of antibody in the joints, we injected BALB/c mice iv with 40 μg of Arthrogen-800, and 21 days post-injection digested the main joints in the hind paws and forepaws (Figure 4A) as described in Materials and Methods and quantified the amount of fluorescent antibody in the digests. In order to account for the effect of tissue lysate on fluorescence, we prepared a standard curve of the antibody in digests of control joints. Arthrogen showed accumulation levels ranging from 5.2 to 16.5 ng per joint (Figure 4B), with hind limb knee showing the highest accumulation, consistent with the NIR images (Figure 4A). Control mouse IgG showed no increase in fluorescence compared to background.

In order to study the microscopical distribution of the antibody in the joints, we scanned the forelimb of a mouse injected with 40 μg of Arthrogen-800 (Figure 3A) with Li-COR Odyssey at the highest resolution (24 μm) and imaged histological sections with a NIR fluorescence microscope. As shown in Figure 5A, there was intense deposition of fluorescence in the joints, including the interphalangeal joints in the paw. In addition, there was some fluorescence in the tendons and in the diaphysis of the bones, consistent with the known collagen type II expression pattern.[8] At the microscopic level (Figure 5B), NIR fluorescence could be detected on the surface of the cartilage and on the endosteal surface

facing the bone marrow. In addition, NIR fluorescence was observed inside chondrocytes (Figure 5B, bottom panel).

Arthrogen is a combination of 5 clones that independently target different epitopes of the CB11 fragment of collagen II. In order to determine the targeting efficiency of Arthrogen compared to a monoclonal antibody, we used a single clone that targets CB11 (hereafter CB11, Figure 6A). CB11 was labeled with IRDye 800, and the labeling efficiency was matched to Arthrogen-800 (Figure 6B).

First, we measured the EC_{50} of binding of both antibodies to a collagen II-coated plate. As shown in Figure 6C, both antibodies bound to collagen II with similar affinity (EC_{50} 4.9 and 3.7 ng/mL for Arthrogen and CB11, respectively), but the monoclonal CB11 antibody showed ~threefold less binding than Arthrogen. Accumulation of antibodies tested ex vivo in the joints of bones taken from the hind limbs (Figure 6D) again showed a ~threefold lower accumulation of CB11. Following intravenous injection of 40 μg/mouse, Arthrogen-800 and CB11–800 showed similar elimination profiles (Figure 6E). Twelve days post-injection, both antibodies showed specific accumulation in the joints (Figure 6F). However, the targeting with CB11 was less efficient; in the joints of greater surface area such as the knee and the shoulder, the accumulation was ~twofold lower than Arthrogen (Figure 6G).

DISCUSSION

In this work, we examined the pharmacokinetics, targeting efficiency, and specificity of a pentaclonal anti-collagen II antibody cocktail and compared it to a monoclonal anticollagen II antibody targeted to the same region of collagen. Many strategies other than collagen II targeting have been explored to target bone, joint tissue, or cells associated with RA. These strategies include complement C2 receptors that bind to complement C3d fragments deposited on the synovial surface,[3] poly-Asp peptide that binds to hydroxyapatite in the bones,[37] PEGylated carbon nanotubes that target monocytes,[38] anti-CD163[39,40] and anti-complement C5aR[41] antibodies that target inflammatory macrophages, anti-CD44 antibody that targets cell adhesion receptors,[42] phage display peptide that binds sinoviocytes,[43,44] and the arginylglycylaspartic acid peptide that targets angiogenic neovasculature in inflamed joints.[45] Although some of these approaches showed efficacy when coupled with therapeutics delivery, to our knowledge, none of these strategies achieved the same level of targeting specificity as Arthrogen. Our data demonstrate highly specific and efficient accumulation of the polyclonal anti-collagen II antibody in the joints of the limbs and spine. Although the pharmacokinetics of the monoclonal antibody was similar to Arthrogen, its targeting efficiency was much lower than Arthrogen. Binding of pentaclonal Arthrogen to multiple epitopes can result in higher target occupancy, which could theoretically explain the observed difference in accumulation, but needs to be investigated further with additional clones of anticollagen antibodies. Although the percentage of bound IgG is lower than reported for tumor-targeted antibodies,[30] it must be kept in mind that we measured the antibody accumulation 3 weeks after the injection, and by that time, some of the antibody and/or dye could already be degraded and excreted. From a therapeutic standpoint, antibody cocktails targeted to multiple epitopes on collagen II could be a promising carrier for

systemically or subcutaneously injected targeted therapeutics to treat rheumatic diseases such as OA and RA. It is generally accepted that nontargeted arthritis therapy causes systemic toxicities.[4–6] For instance, in OA, which lacks disease-modifying therapeutics, anti-inflammatory glucocorticoids and nonsteroidal antiinflammatory drugs (NSAIDs) are in prevalent use along with hyaluronic acid and chondroitin sulfate.[31] Systemic glucocorticoid administration leads to Cushing's syndrome, whereas NSAIDs commonly irritate the gastrointestinal tract, leading to ulceration. Direct IA injection avoids initial systemic exposure, but the dwell time of therapeutics in the articular space is not long[32] and systemic exposure still occurs. Constructs such as nanoencapsulation and hydrogels have been utilized in attempt to maximize drug effects after injection by controlling the rate of release.[33,34] However, IA injections are only feasible when one or two large joints are affected.[35] Therefore, both OA and RA may benefit from improved targeting strategies.

In conclusion, our work suggests that multiclonal anti-collagen antibody cocktails should be explored for targeting of the joints in disease models including RA and eventually for therapeutic delivery.

Supplementary Material

Refer to Web version on PubMed Central for supplementary material.

ACKNOWLEDGMENTS

The study was supported by the NIH grants R01 EB022040, R01 CA194058, and R01 AR051749.

REFERENCES

(1). Lawrence RC; Felson DT; Helmick CG; Arnold LM; Choi H; Deyo RA; Gabriel S; Hirsch R; Hochberg MC; Hunder GG; Jordan JM; Katz JN; Kremers HM; Wolfe F National Arthritis Data, W., Estimates of the Prevalence of Arthritis and Other Rheumatic Conditions in the United States. Part II. Arthritis Rheum. 2008, 58, 26–35. [PubMed: 18163497]

(2). Gottlieb NL; Riskin WG Complications of Local Corticosteroid Injections. JAMA, J. Am. Med. Assoc 1980, 243, 1547–1548.

(3). Kroesen S; Schmid W; Theiler R Induction of an Acute Attack of Calcium Pyrophosphate Dihydrate Arthritis by Intra-Articular Injection of Hylan G-F 20 (Synvisc). Clin. Rheumatol 2000, 19, 147–149. [PubMed: 10791628]

(4). Antoni C; Braun J Side effects of anti-TNF therapy: current knowledge. Clin. Exp. Rheumatol 2002, 20, S152–S157. [PubMed: 12463468]

(5). Singh G; Ramey DR; Morfeld D; Shi H; Hatoum HT; Fries JF Gastrointestinal Tract Complications of Nonsteroidal Anti-Inflammatory Drug Treatment in Rheumatoid Arthritis. A Prospective Observational Cohort Study. Arch. Intern. Med 1996, 156, 1530–1536. [PubMed: 8687261]

(6). Larrar S; Guitton C; Willems M; Bader-Meunier B Severe hematological side effects following Rituximab therapy in children. Haematologica 2006, 91, No. ECR36.

(7). Karsdal MA; Leeming DJ; Henriksen K; Bay-Jensen A-C Biochemistry of Collagens, Laminins and Elastin: Structure, Function and Biomarkers; Elsevier/AP, Academic Press is an imprint of Elsevier: London, United Kingdom; San Diego, CA, United States, 2016; p 238.

(8). Buckley MR; Evans EB; Matuszewski PE; Chen Y-L; Satchel LN; Elliott DM; Soslowsky LJ; Dodge GR Distributions of Types I, Ii and Iii Collagen by Region in the Human Supraspinatus Tendon. Connect. Tissue Res 2013, 54, 374–379. [PubMed: 24088220]

(9). Hughes C; Sette A; Seed M; D'Acquisto F; Manzo A; Vincent TL; Lim N; Nissim A Targeting of Viral Interleukin-10 with an Antibody Fragment Specific to Damaged Arthritic Cartilage Improves Its Therapeutic Potency. Arthritis Res. Ther 2014, 16, R151. [PubMed: 25029910]

(10). Hughes C; Faurholm B; Dell'Accio F; Manzo A; Seed M; Eltawil N; Marrelli A; Gould D; Subang C; Al-Kashi A; De Bari C; Winyard P; Chernajovsky Y; Nissim A Human Single-Chain Variable Fragment That Specifically Targets Arthritic Cartilage. Arthritis Rheum. 2010, 62, 1007–1016. [PubMed: 20131274]

(11). Wahyudi H; Reynolds AA; Li Y; Owen SC; Yu SM Targeting Collagen for Diagnostic Imaging and Therapeutic Delivery. J. Controlled Release 2016, 240, 323–331.

(12). Li Y; Foss CA; Summerfield DD; Doyle JJ; Torok CM; Dietz HC; Pomper MG; Yu SM Targeting Collagen Strands by Photo-Triggered Triple-Helix Hybridization. Proc. Natl. Acad. Sci. U.S.A 2012, 109, 14767–14772. [PubMed: 22927373]

(13). Billinghurst RC; Dahlberg L; Ionescu M; Reiner A; Bourne R; Rorabeck C; Mitchell P; Hambor J; Diekmann O; Tschesche H; Chen J; Van Wart H; Poole AR Enhanced Cleavage of Type Ii Collagen by Collagenases in Osteoarthritic Articular Cartilage. J. Clin. Invest 1997, 99, 1534–1545. [PubMed: 9119997]

(14). Hollander AP; Pidoux I; Reiner A; Rorabeck C; Bourne R; Poole AR Damage to Type Ii Collagen in Aging and Osteoarthritis Starts at the Articular Surface, Originates around Chondrocytes, and Extends into the Cartilage with Progressive Degeneration. J. Clin. Invest 1995, 96, 2859–2869. [PubMed: 8675657]

(15). Hollander AP; Heathfield TF; Webber C; Iwata Y; Bourne R; Rorabeck C; Poole AR Increased Damage to Type Ii Collagen in Osteoarthritic Articular Cartilage Detected by a New Immunoassay. J. Clin. Invest 1994, 93, 1722–1732. [PubMed: 7512992]

(16). Hutamekalin P; Saito T; Yamaki K; Mizutani N; Brand DD; Waritani T; Terato K; Yoshino S Collagen Antibody-Induced Arthritis in Mice: Development of a New Arthritogenic 5-Clone Cocktail of Monoclonal Anti-Type Ii Collagen Antibodies. J. Immunol. Methods 2009, 343, 49–55. [PubMed: 19330909]

(17). Katschke KJ Jr.; Helmy KY; Steffek M; Xi H; Yin J; Lee WP; Gribling P; Barck KH; Carano RAD; Taylor RE; Rangell L; Diehl L; Hass PE; Wiesmann C; van Lookeren Campagne M A Novel Inhibitor of the Alternative Pathway of Complement Reverses Inflammation and Bone Destruction in Experimental Arthritis. J. Exp. Med 2007, 204, 1319–1325. [PubMed: 17548523]

(18). Banda NK; Mehta G; Kjaer TR; Takahashi M; Schaack J; Morrison TE; Thiel S; Arend WP; Holers VM Essential Role for the Lectin Pathway in Collagen Antibody-Induced Arthritis Revealed through Use of Adenovirus Programming Complement Inhibitor Map44 Expression. J. Immunol 2014, 193, 2455–2468. [PubMed: 25070856]

(19). Holers VM; Banda NK Complement in the Initiation and Evolution of Rheumatoid Arthritis. Front. Immunol 2018, 9, 1057. [PubMed: 29892280]

(20). Wang Q; Rozelle AL; Lepus CM; Scanzello CR; Song JJ; Larsen DM; Crish JF; Bebek G; Ritter SY; Lindstrom TM; Hwang I; Wong HH; Punzi L; Encarnacion A; Shamloo M; Goodman SB; Wyss-Coray T; Goldring SR; Banda NK; Thurman JM; et al. Identification of a Central Role for Complement in Osteoarthritis. Nat. Med 2011, 17, 1674–1679. [PubMed: 22057346]

(21). Diamant E; Torgeman A; Ozeri E; Zichel R Monoclonal Antibody Combinations That Present Synergistic Neutralizing Activity: A Platform for Next-Generation Anti-Toxin Drugs. Toxins 2015, 7, 1854–1881. [PubMed: 26035486]

(22). Pasternack JB; Domogauer JD; Khullar A; Akudugu JM; Howell RW The Advantage of Antibody Cocktails for Targeted Alpha Therapy Depends on Specific Activity. J. Nucl Med 2014, 55, 2012–2019. [PubMed: 25349219]

(23). Banda NK; Kraus D; Vondracek A; Huynh LH; Bendele A; Holers VM; Arend WP Mechanisms of Effects of Complement Inhibition in Murine Collagen-Induced Arthritis. Arthritis Rheum. 2002, 46, 3065–3075. [PubMed: 12428251]

(24). Rosenthal EL; Warram JM; de Boer E; Chung TK; Korb ML; Brandwein-Gensler M; Strong TV; Schmalbach CE; Morlandt AB; Agarwal G; Hartman YE; Carroll WR; Richman JS; Clemons LK; Nabell LM; Zinn KR Safety and Tumor Specificity of Cetuximab-Irdye800 for Surgical Navigation in Head and Neck Cancer. Clin. Cancer Res 2015, 21, 3658–3666. [PubMed: 25904751]

(25). Vu VP; Gifford GB; Chen F; Benasutti H; Wang G; Groman EV; Scheinman R; Saba L; Moghimi SM; Simberg D Immunoglobulin Deposition on Biomolecule Corona Determines Complement Opsonization Efficiency of Preclinical and Clinical Nanoparticles. Nat. Nanotechnol 2019, 14, 260–268. [PubMed: 30643271]

(26). Inturi S; Wang G; Chen F; Banda NK; Holers VM; Wu L; Moghimi SM; Simberg D Modulatory Role of Surface Coating of Superparamagnetic Iron Oxide Nanoworms in Complement Opsonization and Leukocyte Uptake. ACS Nano 2015, 9, 10758–10768. [PubMed: 26488074]

(27). Griffin JI; Benchimol MJ; Simberg D Longitudinal Monitoring of Skin Accumulation of Nanocarriers and Biologicals with Fiber Optic near Infrared Fluorescence Spectroscopy (Fonirs). J. Controlled Release 2017, 247, 167–174.

(28). Turner MR; Balu-Iyer SV Challenges and Opportunities for the Subcutaneous Delivery of Therapeutic Proteins. J. Pharm. Sci 2018, 107, 1247–1260. [PubMed: 29336981]

(29). Skalko-Basnet N Biologics: The Role of Delivery Systems in Improved Therapy. Biologics 2014, 8, 107–114. [PubMed: 24672225]

(30). Schneider DW; Heitner T; Alicke B; Light DR; McLean K; Satozawa N; Parry G; Yoo J; Lewis JS; Parry R In Vivo Biodistribution, PET Imaging, and Tumor Accumulation of 86Y- and 111In-Antimindin/RG-1, Engineered Antibody Fragments in LNCaP Tumor-Bearing Nude Mice. J. Nucl. Med 2009, 50, 435–443. [PubMed: 19223400]

(31). Allen KD; Choong PF; Davis AM; Dowsey MM; Dziedzic KS; Emery C; Hunter DJ; Losina E; Page AE; Roos EM; Skou ST; Thorstensson CA; van der Esch M; Whittaker JL Osteoarthritis: Models for Appropriate Care across the Disease Continuum. Best Pract. Res., Clin. Rheumatol 2016, 30, 503–535. [PubMed: 27886944]

(32). Evans CH; Kraus VB; Setton LA Progress in Intra-Articular Therapy. Nat. Rev. Rheumatol 2014, 10, 11–22. [PubMed: 24189839]

(33). Pascual-Garrido C; Rodriguez-Fontan F; Aisenbrey EA; Payne KA; Chahla J; Goodrich LR; Bryant SJ Current and novel injectable hydrogels to treat focal chondral lesions: Properties and applicability. J. Orthop. Res 2018, 36, 64–75. [PubMed: 28975658]

(34). Kang ML; Im G-I Drug Delivery Systems for Intra-Articular Treatment of Osteoarthritis. Expert Opin. Drug Delivery 2014, 11, 269–282.

(35). Habib GS Systemic Effects of Intra-Articular Corticosteroids. Clin. Rheumatol 2009, 28, 749–756. [PubMed: 19252817]

(36). Banda NK; Levitt B; Glogowska MJ; Thurman JM; Takahashi K; Stahl GL; Tomlinson S; Arend WP; Holers VM Targeted Inhibition of the Complement Alternative Pathway with Complement Receptor 2 and Factor H Attenuates Collagen Antibody-Induced Arthritis in Mice. J. Immunol. 2009, 183, 5928–5937. [PubMed: 19828624]

(37). Kasugai S; Fujisawa R; Waki Y; Miyamoto K; Ohya K Selective drug delivery system to bone: small peptide (Asp)6 conjugation. J. Bone Miner. Res 2000, 15, 936–943. [PubMed: 10804024]

(38). Sacchetti C; Liu-Bryan R; Magrini A; Rosato N; Bottini N; Bottini M Polyethylene-Glycol-Modified Single-Walled Carbon Nanotubes for Intra-Articular Delivery to Chondrocytes. ACS Nano 2014, 8, 12280–12291. [PubMed: 25415768]

(39). Graversen JH; Svendsen P; Dagnæs-Hansen F; Dal J; Anton G; Etzerodt A; Petersen MD; Christensen PA; Møller HJ; Moestrup SK Targeting the Hemoglobin Scavenger Receptor Cd163 in Macrophages Highly Increases the Anti-Inflammatory Potency of Dexamethasone. Mol. Ther. 2012, 20, 1550–1558. [PubMed: 22643864]

(40). Eichendorff S; Svendsen P; Bender D; Keiding S; Christensen EI; Deleuran B; Moestrup SK Biodistribution and Pet Imaging of a Novel [68ga]-Anti-Cd163-Antibody Conjugate in Rats with Collagen-Induced Arthritis and in Controls. Mol. Imaging Biol 2015, 17, 87–93. [PubMed: 25053229]

(41). Mehta G; Scheinman RI; Holers VM; Banda NK A New Approach for the Treatment of Arthritis in Mice with a Novel Conjugate of an Anti-C5ar1 Antibody and C5 Small Interfering Rna. J. Immunol 2015, 194, 5446–5454. [PubMed: 25917104]

(42). Mott PJ; Lazarus AH Cd44 Antibodies and Immune Thrombocytopenia in the Amelioration of Murine Inflammatory Arthritis. PLoS One 2013, 8, No. e65805.

(43). Mi Z; Lu X; Mai JC; Ng BG; Wang G; Lechman ER; Watkins SC; Rabinowich H; Robbins PD Identification of a Synovial Fibroblast-Specific Protein Transduction Domain for Delivery of Apoptotic Agents to Hyperplastic Synovium. Mol. Ther 2003, 8, 295–305. [PubMed: 12907152]

(44). Vanniasinghe AS; Manolios N; Schibeci S; Lakhiani C; Kamali-Sarvestani E; Sharma R; Kumar V; Moghaddam M; Ali M; Bender V Targeting Fibroblast-Like Synovial Cells at Sites of Inflammation with Peptide Targeted Liposomes Results in Inhibition of Experimental Arthritis. Clin. Immunol 2014, 151, 43–54. [PubMed: 24513809]

(45). Scheinman RI; Trivedi R; Vermillion S; Kompella UB Functionalized Stat1 Sirna Nanoparticles Regress Rheumatoid Arthritis in a Mouse Model. Nanomedicine 2011, 6, 1669–1682. [PubMed: 22087799]

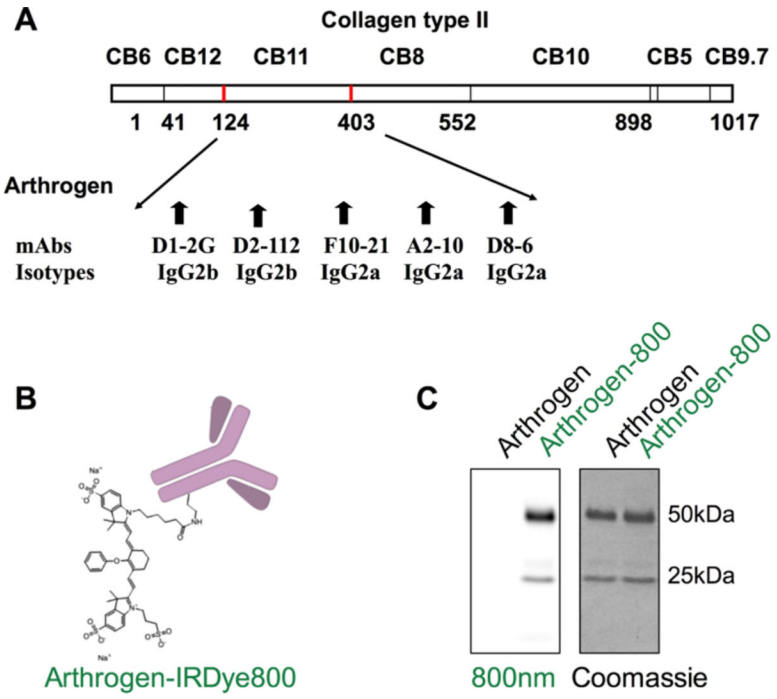

Figure 1.

Fluorescent labeling of Arthrogen: (A) CB11 fragment of collagen type II targeted by Arthrogen (5 different epitopes); (B) labeling with IRDye 800 on the lysine groups of Arthrogen. The actual labeling was 2 dye molecules per IgG for this experiment; and (C) reducing SDS-PAGE shows labeling of both heavy and light chains of the antibody.

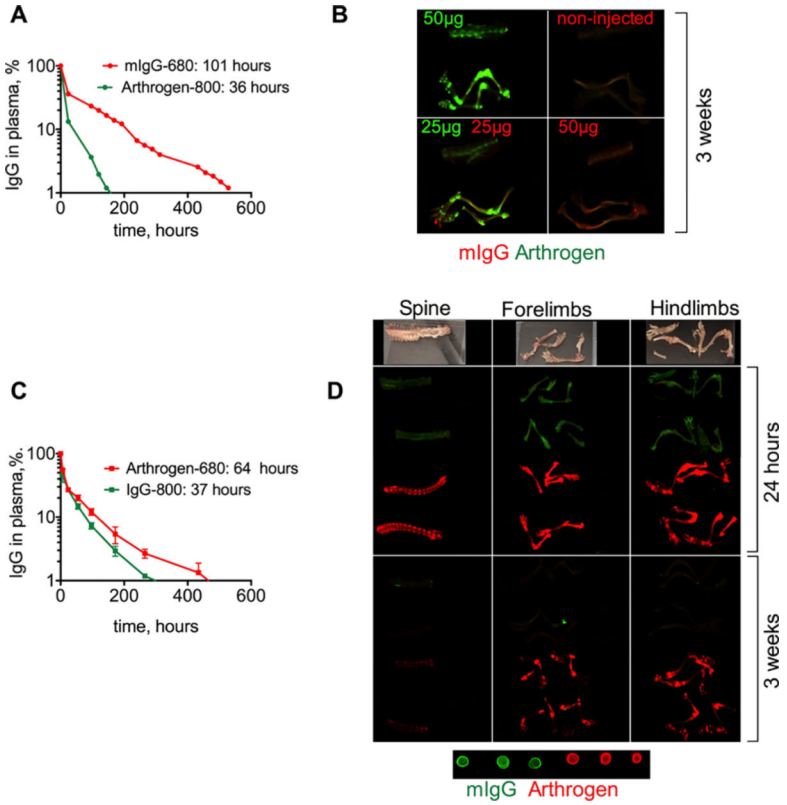

Figure 2.

Accumulation of Arthrogen in joints of healthy BALB/c mice after iv injection: (A) circulation profile and pharmacokinetic data (slow phase) of Arthrogen-800 and control mouse IgG-680. The experiment was repeated twice; (B) images of dissected bones of Arthrogen-injected (green) and mIgG-injected (red) mice. Arthrogen clearly localized in the joints. In each panel, from top to bottom: spine, hind limb, and forelimb. Contrast in 700 and 800 nm channels was adjusted to the same extent for all mice; (C) circulation profile and pharmacokinetic data (slow phase) of Arthrogen-680 and control mouse IgG-800; (D) images at 24 h (perfused mouse) and 3 weeks post-injection show fast and specific accumulation of Arthrogen in the joints and the spine. In this experiment, the labeling dyes were swapped, mIgG (green) and Arthrogen (red). Dots show 100× dilution of each antibody applied on nitrocellulose membrane and scanned together with the organs. The photographs and scans of all bones and major organs are in Figure S2.

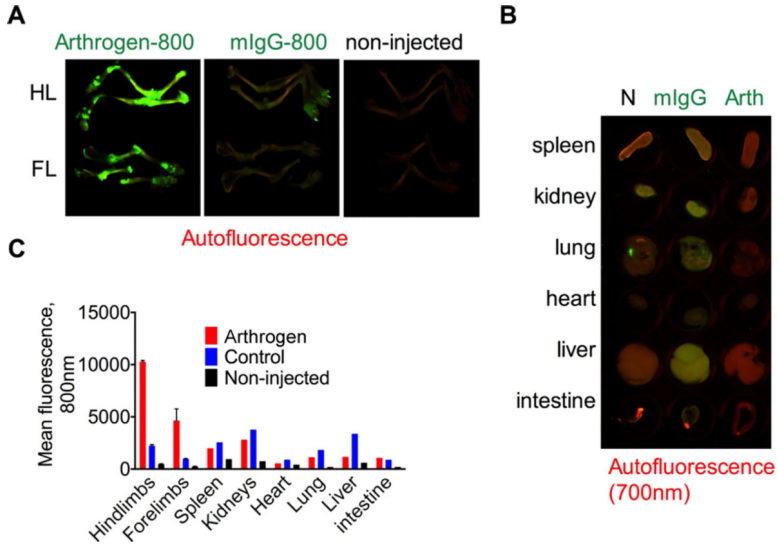

Figure 3.

Specificity of Arthrogen accumulation in joints of healthy BALB/c mice following subcutaneous injection: (A) images of dissected bones of Arthrogen-800-injected and control mIgG-800-injected mice. Auto fluorescence was scanned at 700 nm. FL = forelimb, HL = hind limb; (B) images of control organs (N = non-injected, IgG = control mIgG-800, and Arth = Arthrogen-800); (C) mean fluorescence of organs as determined from grayscale images. Contrast in 700 and 800 nm channels was adjusted to the same extent for all mice and for all organs and bones. The experiment was repeated twice.

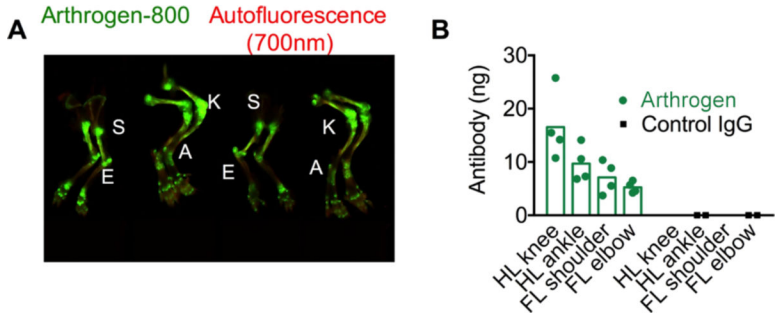

Figure 4.

Distribution of Arthrogen in different joints: joints were dissected, homogenized, digested with proteinase K, and the amount of fluorescence was quantified as described in Materials and Methods (n = 2 BALB/c mice, 2 joints per group). (A) Limbs of mice 3 weeks after injection. S = shoulder, E = elbow, K = knee, and A = ankle; (B) quantification in the dissected joints.

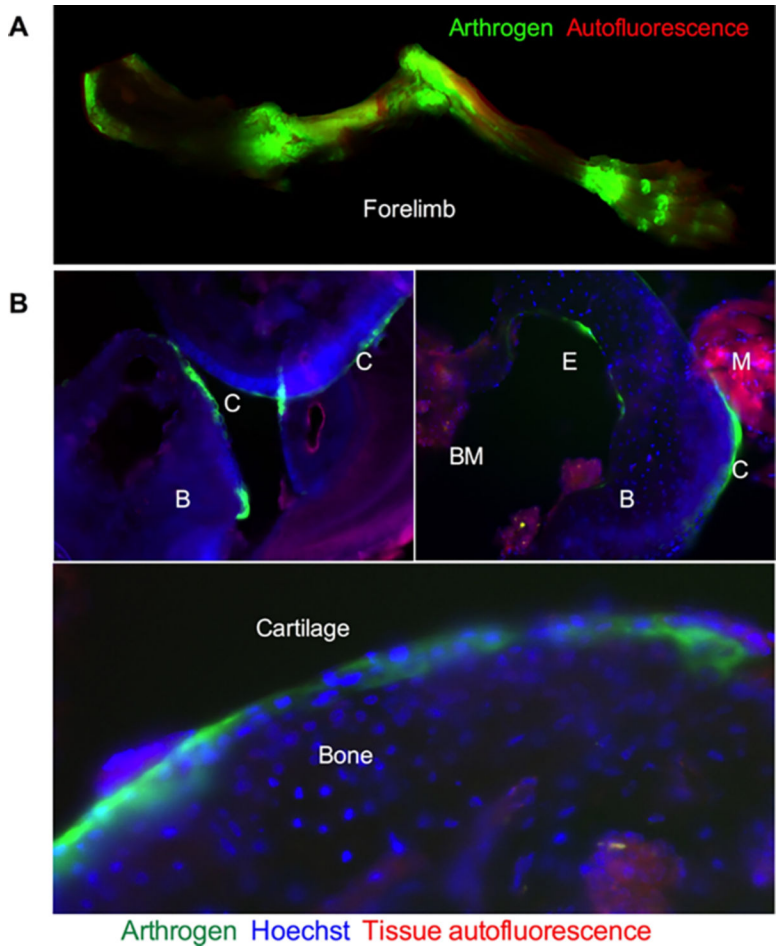

Figure 5.

High-resolution NIR imaging of the bones after Arthrogen injection: (A) forelimb from Arthrogen-injected mouse (Figure 3) scanned at 24 μm resolution with Li-COR. The high-resolution image shows accumulation in the joints, tendons, and to some extent in the diaphysis of the bone; (B) histological sections of knee and elbow joints of Arthrogen-injected mouse imaged with a NIR microscope. The antibody not only accumulated in the cartilage (C) but also was observed on the endosteal surface (E). B = bone, BM = bone marrow, and M = for muscle. High magnification (bottom) shows accumulation in chondrocytes in the cartilage. Red autofluorescence (rhodamine filter) highlights muscle and bone marrow.

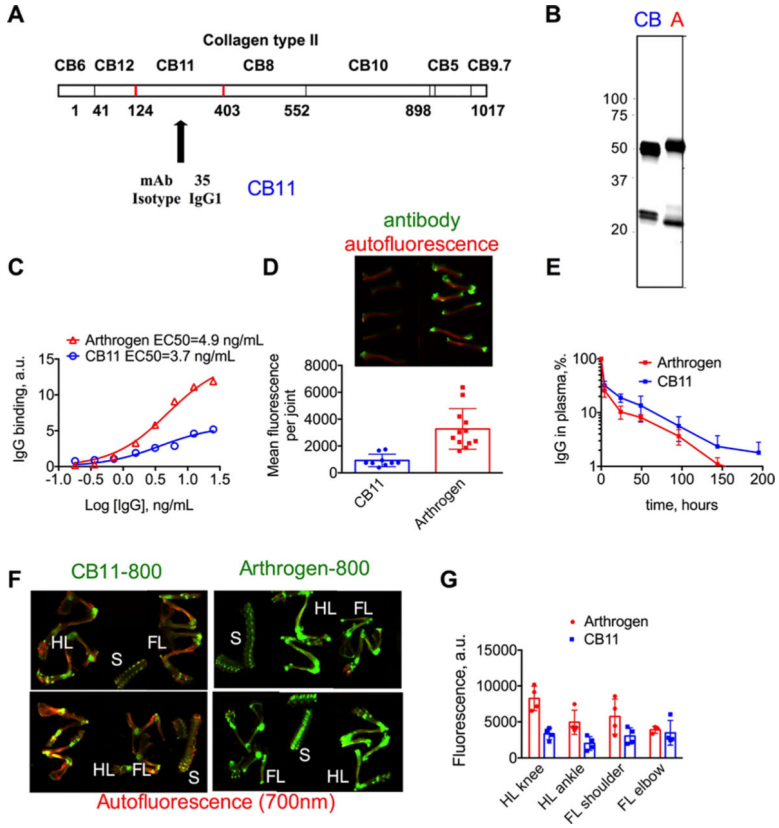

Figure 6.

Accumulation of monoclonal Ab vs Ab cocktail in the joints of BALB/c mice after iv injection: (A) epitope of CB11 domain of collagen II targeted by the CB11 monoclonal antibody; (B) NIR image of SDS-PAGE gel of both CB11–800 and Arthrogen-800 showing similar labeling efficiency (100 ng of each Ab was loaded); (C) collagen binding assay shows binding to collagen with similar affinity but lower efficiency for CB11–800; (D) images of bones exposed to CB11–800 and Arthrogen-800 ex vivo and quantification of mean fluorescence of joints at 800 nm; (E) CB11 and Arthrogen show similar rates of clearance determined by plasma fluorescence at 800 nm; (F) images of dissected bones of CB11–800 and Arthrogen-800 iv-injected mice. HL = hind limb, FL = forelimb, and S = spine. The signal in 700 nm (autofluorescence) was enhanced to make the bones visible; (G) quantification of total fluorescence of joints in (F) shows higher accumulation of Arthrogen-800 in most joints.